

# Experimental Investigation of the Flow Field around NACA0012 Airfoil

Onur Yemenici 

**Abstract:** In this study, an experimental investigation of the flow field around NACA0012 airfoil was carried out in a wind tunnel under the effects of the Reynolds number and angle of attack. The Reynolds number based on the chord length of airfoil and the attack angle was varied from  $9.7 \times 10^4$  to  $1.9 \times 10^5$  and 0 to  $14^\circ$  respectively. Mean velocities were measured by a constant temperature anemometer and static pressures by a micro-manometer. The results showed that the pressure and lift coefficients displayed a strong dependence on Reynolds number and attack angle.

**Index Terms:** Airfoil, attack angle, pressure coefficient, lift coefficient

## I. INTRODUCTION

The aerodynamic characteristics of airfoils at a small chord Reynolds number (less than  $5 \times 10^5$ ) are becoming increasingly important from both fundamental and industrial point of view, due to recent developments in small wind turbines, small unmanned aerial vehicles, micro-air vehicles, as well as researches on bird/insect flying aerodynamics. Therefore, there have been several previous investigations on the side mirrors such as, Ahmed et al. [1] carried out a computational study into the flow field developed around a cascade of NACA0012 airfoils. Genc et al. [2] investigated flow over an airfoil without and with a leading-edge slat at a transitional Reynolds number. A numerical simulation of the flow field around a cascade of NACA0012 airfoils-effects of solidity and stagger was performed by Yilbas et al. [3]. The flow transients associated with controlled reattachment and separation of the flow over a stalled airfoil was investigated by Amitay and Glezer [4]. Singh et al. [5] designed a low Reynolds number airfoil for applications in small horizontal axis wind turbines to achieve better startup and low wind speed performance.

Experimental investigations on the effects of divergent trailing edge and Gurney flaps on a supercritical airfoil were carried out by Li et al. [6]. Ahmed and Sharma [7] performed an investigation on the aerodynamics of a symmetrical airfoil in ground effect. Single and multi-point optimization of an airfoil using gradient method was performed by Mirzaei et al [8]. Mueller et al. [9] investigated the influence of free-stream disturbances on low Reynolds number airfoil experiments. Eisenbach and Friedrich studied on large-eddy simulation of flow

separation on an airfoil at a high angle of attack and  $Re=10^6$ . Analysis of ground effects on aerodynamic characteristics of airfoils using boundary layer approximation was carried out by Takahashi et al. [10]. Yen and Huang [11] studied on the Reynold number effects on flow characteristics and aerodynamic performances of a swept-back wing. Tuck and Soria [12] performed separation control on a NACA0015 airfoil using a micro jet.

In this study, the measurements were carried out for the Reynolds number of  $9.7 \times 10^4$  and  $1.9 \times 10^5$  and attack angle of 0 to  $14^\circ$  with  $2^\circ$  intervals to investigate the effects of these parameters on aerodynamic characteristics of NACA0012 airfoil.

## II. EXPERIMENTAL PROCEDURE AND EQUIPMENT

The blowing-type, low-speed wind tunnel which is consist of a metal duct, a honey comb, a nozzle, a straightening duct and a test section was used to measurements, as shown in Fig. 1. The honey comb with a cross-sectional area of  $305 \times 305 \text{ mm}^2$  and the nozzle with 1.5:1 contraction ratio was used to obtain smooth streamlines and to reduce turbulent level and to prevent boundary layer separations and accelerate air flow, respectively. The contractions effects of the nozzle were eliminated by the straightening duct. The tunnel has 30 m/s the maximum air velocity at the inlet of the test section with a turbulent intensity of 0.7%, run by a 5.7 kW axial blower and flow rates were adjusted by a butterfly valve within the tunnel. The plexiglass test section has an initial area of  $200 \times 305 \text{ mm}^2$  and provided full visibility of the flow area.



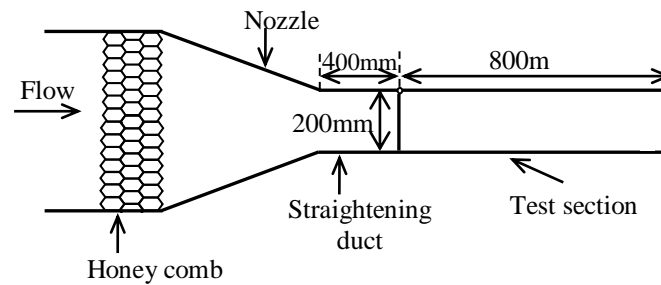


Fig. 1. Wind tunnel

The mean velocities of the tunnel that were obtained at a sampling frequency of 2500 Hz and low-pass filter frequency of 1250 Hz were measured by DANTEC digital constant temperature anemometer, 55P11 probes and a calibration device. The static pressure measurements were carried out by using pressure tappings with a diameter of 0.5 mm and were recorded by a micro-manometer.

All experiments were conducted using a wool NACA0012 airfoil with a chord length of 152 mm (C)

and a span of 305 mm which was mounted in the middle of the test section of the wind tunnel, as shown in Fig. 2. The flow field around the airfoil was ideally free from 3D effects due to equal spanwise length with test section. The mean static pressure measurements of the suction side and pressure side of the airfoil were performed at both 10 location, as presented in Fig. 3. The intended angles of attack ( $\alpha$ ) were also obtained by an angle adjuster.



Fig. 2. Experimental set up of the airfoils.

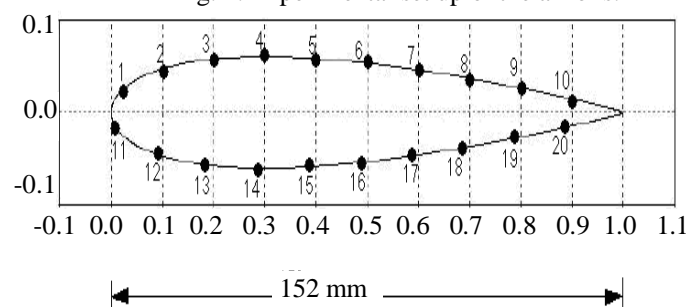


Fig. 3. The airfoil pressure tappings

Pressure and lift coefficients are derived by

$$C_p = \frac{P - P_0}{0.5\rho U^2} \text{ and}$$

$$C_L = \frac{L}{0.5\rho U^2 A}, \text{ respectively, where}$$

- P: static pressure measured at pressure tappings
- $P_0$ : static pressure of free stream
- U: free stream velocity
- $\rho$ : density
- L: lift force
- A: effect area

The maximum uncertainties in the velocity and pressure are found to be  $\pm 2.2\%$  and  $3.8\%$ , respectively.

**III. RESULTS AND DISCUSSION**

The measurements carried out for free stream velocity of 10 and 20 m/s, corresponding to the chord length Reynolds number ( $Re_c$ ) of  $9.7 \times 10^4$  and  $1.9 \times 10^5$ , respectively.

The pressure distribution of the NACA0012 airfoil at angles of  $\alpha=0-12^\circ$  and  $Re_c=9.7 \times 10^4$  are given in Fig. 4. For all the angles of attack, the pressure coefficient had a

large suction peak at the suction surface near the leading edge, and followed by a gradual increase in pressure. The stall point of the pressure side was obtained near the leading edge, where the pressure coefficient attained maximum value, as explained by Yilbas et al. [3]. At  $\alpha=0^\circ$ , the pressure variation over the suction and pressure side of the airfoil showed a symmetric distribution, as expected. Suction peaks of the suction side were in the range of -1.5 and -3.5 from the attack angle of  $0^\circ$  to  $12^\circ$ .

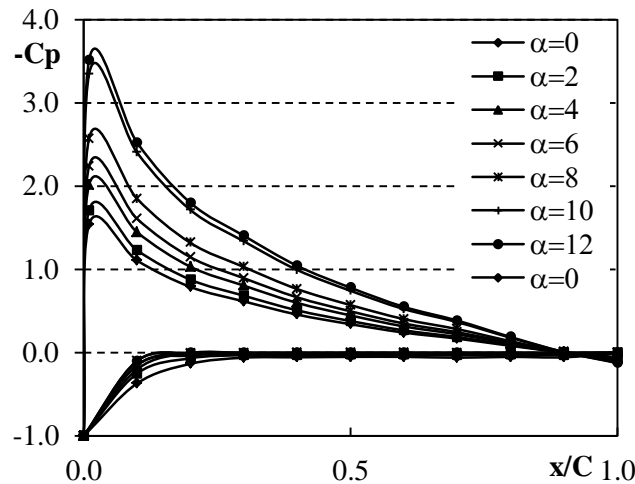


**Fig. 4.** Pressure distributions of suction and pressure side of the airfoil at  $Re_c=9.7 \times 10^4$ .

A slight increase and then subsequent decrease was obtained in the  $C_p$  curves of suction surface in Fig. 6, similar to the curves of smaller Reynolds number and the findings of Boutilier and Yarusevych [13]. It can be said from the curves that the boundary layer developed after peak suction from the leading edge to trailing edge, as the pressure slowly increased. The maximum  $C_p$  values of the pressure side of the airfoil changed from -0.1 to

-0.0005 up to trailing edge at  $\alpha=0^\circ$  and -0.4 to -0.004 at  $\alpha=12^\circ$ .  $C_p$  values increased with attack angle as smaller Reynolds number results. The separation and reattachments couldn't determine from the pressure measurements due to the fact that the pressure tappings cannot be completely flush along the pressure and suction side of the airfoil.

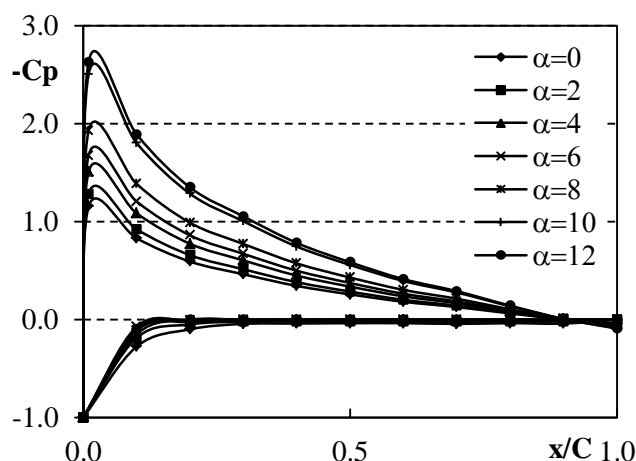


**Fig. 5.** Pressure distributions of suction and pressure side of the airfoil at  $Re_c=1.9 \times 10^5$ .

Lift characteristics of airfoil at different Reynolds numbers is given in Fig. 7. For lower angles of attack, the  $C_L$ - $\alpha$  curve is nearly linear, in a good agreement with the

result of Genç et al. [14]. The  $C_L$  increased monotonously with angle attack and reached the maximum at the angle attack of  $12^\circ$  and  $13^\circ$  at  $Re_c=9.7 \times 10^4$  and  $1.9 \times 10^5$ , respectively. This result

showed the occurrence of the stall at  $\alpha=12^0$  and  $13^0$  and the angle of stall increased with Reynolds number. The maximum  $C_L$  defined at the stall angle and showed vary

with Reynolds number due to viscous effects, which had 10% bigger values at  $Re_C=1.9 \times 10^5$ .

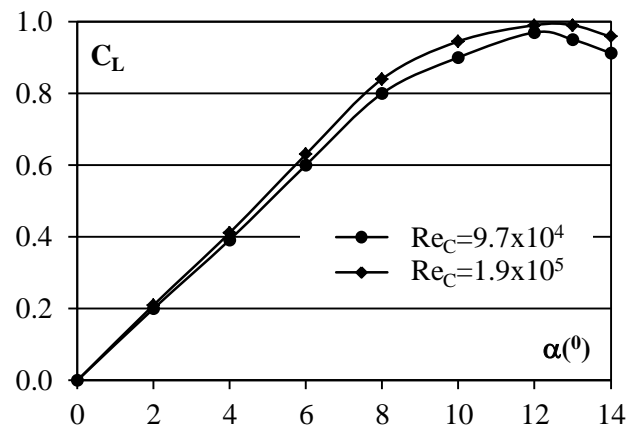


Fig. 6. Lift characteristics of airfoil at different Reynolds numbers.

#### IV. CONCLUSION

The measurements were performed for  $97000 \leq Re_C \leq 190000$  and  $0^0 \leq \alpha \leq 14^0$  around NACA0012 airfoil. The pressure coefficient of the suction side of the airfoil initially increased near the leading edge and then showed a monotonously decrease up to trailing edge for all angle of attack. A symmetric pressure distribution was obtained along the suction and pressure side of the airfoil at zero attack angles. The  $C_p$  curves showed similar distributions both Reynolds number. The lift coefficients reached maximum values at stall angle which was  $12^0$  and  $13^0$  at  $Re_C=9.7 \times 10^4$  and  $1.9 \times 10^5$ , respectively. The angles of stall and lift coefficients increased with Reynolds number.

#### REFERENCES

[1] N. Ahmed and B.S. Yilbas and M.O. Budair, "Computational study into the flow field developed around a cascade of NACA 0012 airfoils", Computer methods in applied mechanics and engineering, vol.167, 1998, pp. 17-32.  
 [2] M.S. Genç and İ. Karasu and H.H. Açıkel, "An experimental study on aerodynamics of NACA2415 aerofoil at low Re numbers", Experimental Thermal and Fluid Science, vol.39, 2012, pp. 252-264.  
 [3] M.S.H. Boutillier and S. Yarusevych, "Parametric study of separation and transition characteristics over an airfoil at low Reynolds numbers", Exp. Fluids., vol.52, 2012, pp. 1491-1506  
 [4] A. Tuck and J. Soria, "Separation control on a NACA 0015 airfoil using a 2D micro ZNMF jet", Aircraft Engineering and Aerospace Technology, vol.80, 2008, pp. 175-180.

[5] S.C. Yen and L.C. Huang, "Reynolds number effects on flow characteristics and aerodynamic performances of a swept- back wing", Aerospace Science and Technology, vol.15, 2011, pp. 155-164.  
 IV. [6] Y. Takahashi and M. Kikuchi and K. Hirano, "Analysis of Ground Effects on Aerodynamic Characteristics of Aerofoils Using Boundary Layer Approximation", JSME International Journal Series B Fluids and Thermal Engineering, vol.49, 2006, pp. 401-409.  
 [7] T.J. Mueller and L.J. Pohlen and P.E. Conigliaro and B.J. Jansen and Jr, "The Influence of Free-Stream Disturbances on Low Reynolds Number Airfoil Experiments", Experiments in Fluids, vol.1, 1983, pp. 3-14.  
 [8] M. Mirzaei and S.N.Hosseini and J. Roshanian, "Single and multi-point optimization of an airfoil using gradient method", Aircraft Engineering and Aerospace Technology, vol.79, 2007, pp. 611-620.  
 [9] M.R.Ahmed and S.D. Sharma, "An investigation on the aerodynamics of a symmetrical airfoil in ground effect", Experimental Thermal and Fluid Science, vol.29, 2005, pp. 633-647.  
 [10] Y.C. Li and J.J. Wang and J. Hua, "Experimental investigations on the effects of divergent trailing edge and Gurney flaps on a supercritical airfoil", Aerospace Science and Technology, vol.11, 2007, pp. 91-99.  
 [11] R.K. Singh and M.R. Ahmed and M.A. Zullah and Y.H. Lee, "Desing of a low Reynolds number airfoil for small horizontal axis wind turbines", Renewable Energy, vol.42, 2012, pp. 66-76.  
 [12] M. Amitay and A. Glezer, "Controlled transients of flow reattachment over stalled airfoils", International journal of heat and fluid flow, vol.23, 2002, pp. 690-699.  
 [13] B.S. Yilbas and M.O. Budair and N. Ahmed, "Numerical simulation of the flow field around a cascade of NACA 0012 airfoils-effects of solidity and stagger", Computer methods in applied mechanics and engineering, vol.158, 1998, pp. 143-154.  
 [14] M.S. Genç and Ü. Kaynak and G.D.Lock, "Flow over an aerofoil without and with a leading- edge slat at a transitional Reynolds number", Proc IMechE, Part G- Journal of Aerospace Engineering, vol.223, 2009, pp. 217-231.